

## Chapter 1

# Manganites

### 1.1 General properties

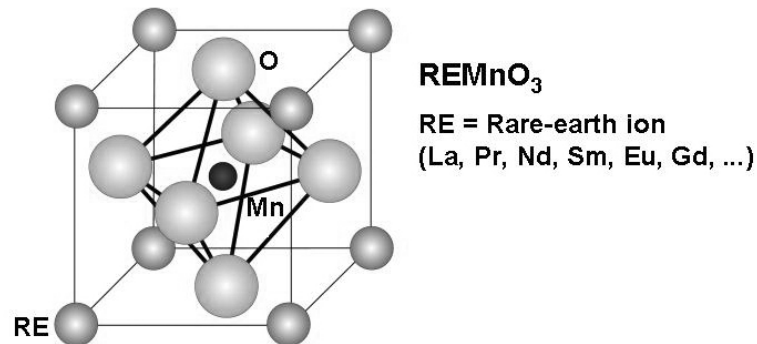


Figure 1.1: *REMnO<sub>3</sub> perovskite crystal structure.*

The rare-earth manganites crystallize in the cubic perovskite structure with the general notation  $\text{REMnO}_3$ , as shown in Fig.1.1.  $\text{LaMnO}_3$  is the parent compound of rare-earth manganites. The La ion (RE ion) occupies the corner site of the cube, the Mn ion occupies the center of the cubic structure and the oxygen ions surround the manganese ion in the form of an octahedron. In the ideal perovskite structure the bond lengths between the La, Mn and O ions have the ratio  $\langle \text{La} - \text{O} \rangle / \langle \text{Mn} - \text{O} \rangle = \sqrt{2}$ . In the ionic model the bond lengths are defined by the ionic radii. The tolerance factor which is a measure of the deviations from the ideal cubic perovskite structure, is calculated from the ionic radii of the lattice sites in a perovskite structure [Goldschmidt 58],

$$\text{tolerance factor} : t = \frac{r(\text{RE}) + r(\text{O})}{\sqrt{2} [r(\text{Mn}) + r(\text{O})]}. \quad (1.1)$$

where  $r(\text{RE})$ ,  $r(\text{Mn})$  and  $r(\text{O})$  are the averaged ionic radii at sites RE, Mn and of the oxygen ion, respectively. The pseudo-cubic perovskite structure stabilizes when the tolerance factor has the value  $t$  with  $0.89 < t < 1.02$ . The deviation from the tolerance factor  $t = 1$  gives the distorted perovskite structure in the form of orthorhombic and rhombohedral structures. The parent compound  $\text{LaMnO}_3$  crystallizes into the orthorhombic structure with the tolerance factor  $t \approx 0.89$ . The perovskite structure allows a wide variety of doping at both RE and Mn ion sites. In this thesis, the La site is doped with alkaline earth metal ions  $\text{Ca}^{2+}$ ,  $\text{Sr}^{2+}$ ,  $\text{Pb}^{2+}$  and the Mn site is doped with  $\text{Ta}^+$ ,  $\text{W}^+$  and  $\text{Ru}^+$ . In the parent  $\text{LaMnO}_3$  compound, Mn is in the 3+ ionic state, i.e it has 4 electrons in the 3d shell.

The ground state of the parent  $\text{LaMnO}_3$  compound is an A-type antiferromagnetic insulator. Within the layers, the spins are coupled ferromagnetically and the layers in the orthorhombic structure are coupled antiferromagnetically. There are two types of magnetic exchange interactions present in manganites, known as double exchange and super exchange interactions. Zener introduced the concept of ferromagnetic double exchange interaction [Zener 51a, Zener 51b], assuming two simultaneous electron transfers: one electron from  $\text{Mn}^{3+}$  to an overlapping O2p orbital and a second electron from O2p orbital to the adjacent  $\text{Mn}^{4+}$  ion. The superexchange interactions were introduced by Goodenough [Goodenough 51]. It is defined as the coupling between the  $\text{Mn}^{3+} - \text{Mn}^{3+}$  ions via O2p orbitals, depending strongly upon the orientation of the  $e_g$  orbitals. The magnetic ground state of the manganites depends upon the competition between these two magnetic exchange interactions. In order to explain the ground state nature of the parent compound  $\text{LaMnO}_3$ , the strong Jahn-Teller effect of the  $\text{Mn}^{3+}$  ion needs to be considered. The Jahn-Teller effect is defined as the degeneracy of the  $\text{Mn}^{3+} e_g$  orbital state being lifted by the distortion of the oxygen octahedron in the lattice.

The antiferromagnetic structure is well explained by superexchange interactions. Ferromagnetic  $\text{Mn}^{3+} - \text{O}2\text{p} - \text{Mn}^{3+}$  superexchange dominates within the parallel lattice planes, with neighboring planes coupling antiferromagnetically. The compound remains in the insulator state because it needs an energy of about

1.2 eV (Jahn-Teller splitting energy) to jump from the lower  $e_g$  orbital to the upper energy level of the neighboring  $e_g$  orbital.

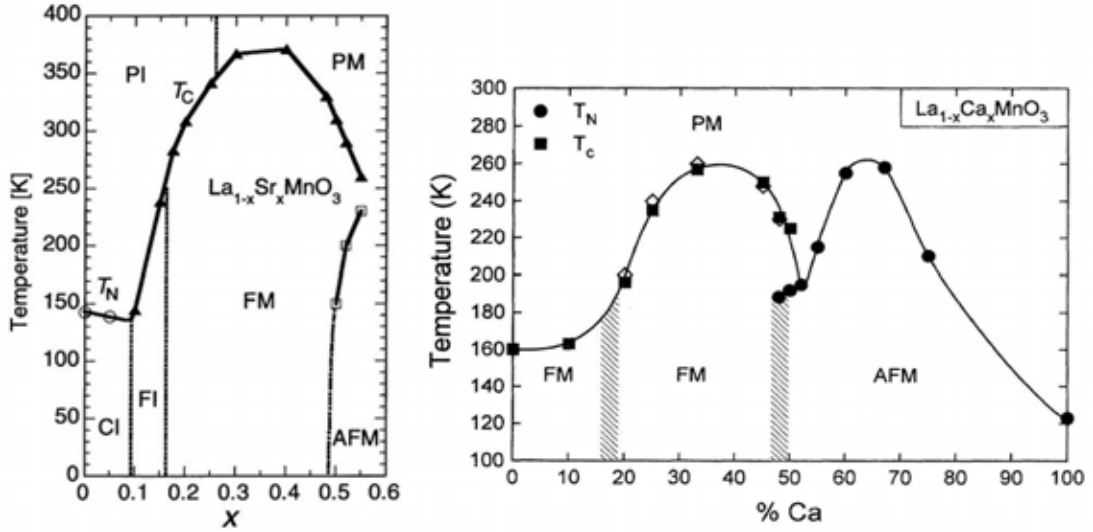


Figure 1.2: Phase diagrams of  $La_{1-x}Sr_xMnO_3$  [Tokura 99, Urushibara 95] and  $La_{1-x}Ca_xMnO_3$  [Schiffer 95] manganite compounds ( $T_N$ ,  $T_C$ : Neel, Curie temperatures; PI: Paramagnetic Insulator, PM: Paramagnetic Metal, CI: Charge Insulator, FI: Ferromagnetic Insulator, FM: Ferromagnetic Metal, AFM: Antiferromagnetic Metal, CO: Charge Ordered, AF: Antiferromagnetic, CAF: Canted Antiferromagnet)

By varying the composition of the divalent alkaline earth metals at the La site, a rich variety of phase diagrams is produced, as shown for the Sr, Ca doped manganites in Fig.1.2. The ground state of the manganite material basically depends upon the number of doped charge carriers and the average ionic radii on La and Mn lattice sites. Many ground states are observed for the doped manganites which include ferromagnetic metals, antiferromagnetic insulators, ferromagnetic insulators, antiferromagnetic metals (rare), glassy insulators and canted magnetic insulators. In this thesis, essentially the ferromagnetic metallic region is considered, as all our compounds are doped according to the ferromagnetic metallic region. The divalent ion ( $Sr^{2+}$ ,  $Ca^{2+}$ ) introduces an equal number of  $Mn^{4+}$  ions into the compound. The compound becomes a ferromagnetic metal due to the fact that the localized electrons become delocalized by moving between  $Mn^{3+}$  and  $Mn^{4+}$  ions via O2p orbital, conserving the spin of the electron. From the Zener ferromagnetic double exchange concept, it is assumed that the compound becomes metallic only when the neighboring spins are ferromagnetically coupled.

The schematic diagram of the double exchange interaction between  $Mn^{3+}$  and  $Mn^{4+}$  via the O2p orbital is shown in Fig.1.3.

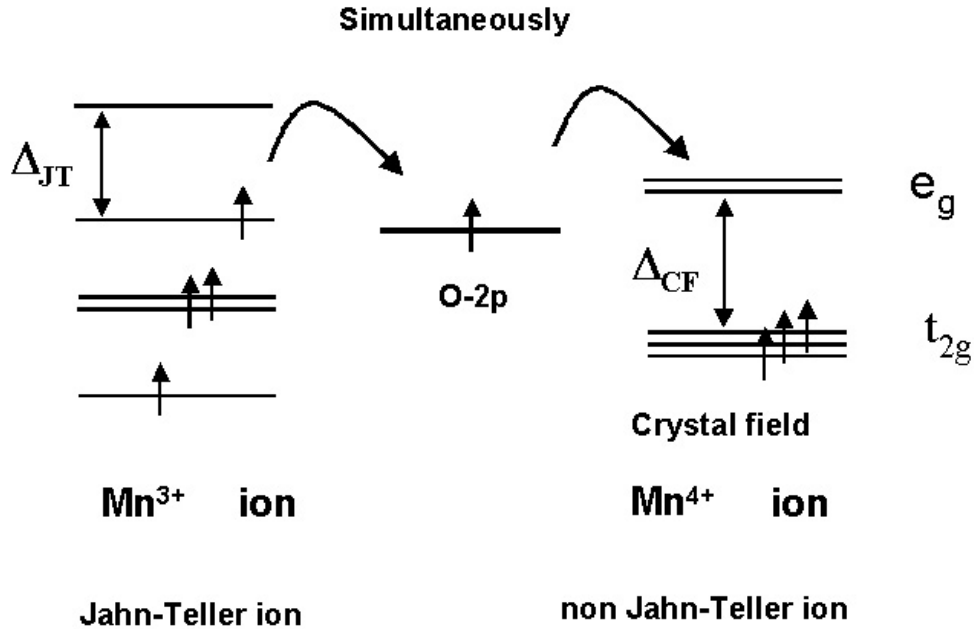


Figure 1.3: Schematic diagram of double exchange interaction in manganites. The position of the oxygen orbital is arbitrary.  $\Delta_{CF}$ ,  $\Delta_{JT}$  denote the crystal field splitting energy and Jahn-Teller splitting energy respectively.

## 1.2 Intrinsic electric transport

In this section, the electric transport properties of single crystalline ferromagnetic manganites are discussed. The properties remain the same for high quality epitaxial films of sufficient thickness. The ferromagnetic manganites are well known for their extraordinary transport properties such as colossal magnetoresistance (CMR) and its half-metallic nature below the Curie temperature. The half-metallic nature for the manganites was predicted from band structure calculations. The conduction electrons below the ferromagnetic Curie temperature  $T_C$  are polarized in the spin up direction. A schematic diagram of a half metal is shown in Fig.1.4(a). The large tunneling magnetoresistance observed for manganites [Bowen 03] of the type  $La_{1-x}Sr_xMnO_3$  gives evidence for the large spin polarization of tunneling electrons.

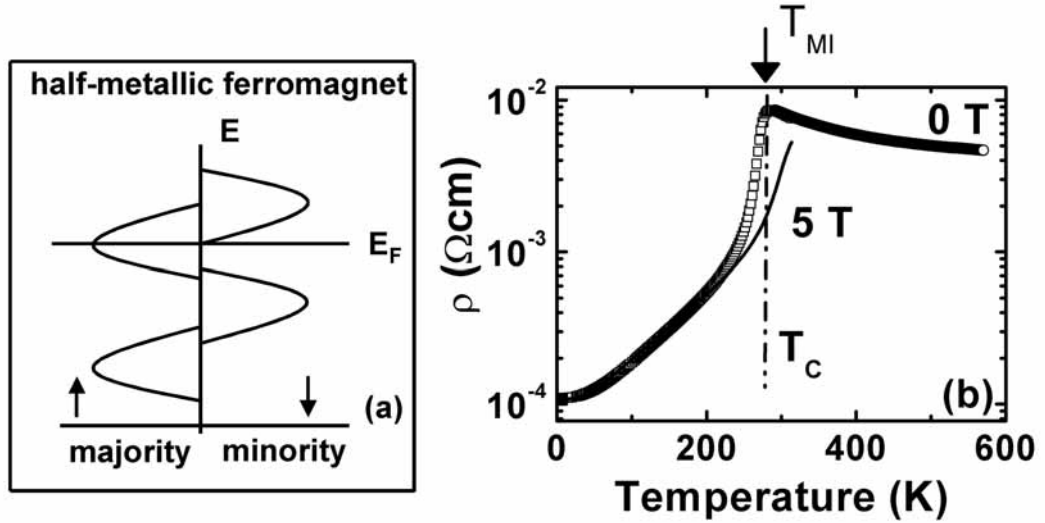


Figure 1.4: (a) Schematic band diagram of a half metallic ferromagnet,  $E_F$  is the Fermi energy (b) Temperature-dependent resistivity of a ferromagnetic  $\text{La}_{0.7}\text{Ca}_{0.3}\text{MnO}_3$  epitaxial film on  $\text{LaAlO}_3$  substrate, measured in zero and in 5 T magnetic field;  $T_{MI}$ ,  $T_C$  denote the metal-insulator transition temperature and the ferromagnetic Curie temperature [Dörr 06].

In Fig.1.4(b), the temperature dependence of resistance in zero field and in 5 T magnetic field of a  $\text{La}_{0.7}\text{Ca}_{0.3}\text{MnO}_3$  epitaxial manganite film is shown. The increase in resistance with respect to temperature is referred as metallic and the decrease in resistance with rising temperature is referred as insulating. The transition from metallic to insulator nature is indicated in Fig.1.4(b) as  $T_{MI}$ , the metal-insulator transition temperature.  $T_{MI}$  is very near to the magnetic Curie temperature ( $T_C$ ).

Viret et al. [Viret 97] derived a model based on magnetic localization in order to describe the temperature dependence of the ferromagnetic metallic state. The magnetic localization model describes very well the temperature dependence of the  $\text{La}_{0.7}\text{Ca}_{0.3}\text{MnO}_3$ . In the paramagnetic insulator state  $T > T_C$ , polaron hopping  $\rho(T) = AT \exp[(E_{hop})/k_B T]$  [Worledge 96], Mott variable range hopping  $\rho(T) = A \exp[(E/k_B T)^{0.25}]$  [Coey 95, Coey 99] and simple thermal activation  $\rho(T) = A \exp(E/k_B T)$  models are widely used to describe the transport behavior.

The magnetoresistance (MR) is maximum close to the metal-insulator transition temperature ( $T_{MI}$ ). The resistance measured in an applied field may decrease by several orders of magnitude compared to zero magnetic field, as shown in Fig.1.4(b). The MR is found to be maximum for the lower  $T_{MI}$  manganites

and the drop in resistance in magnetic field can reach up to ten orders of magnitude. This anomalous decrease in resistance with respect to applied field is known as CMR (colossal magnetoresistance). Towards low temperatures the MR decreases and vanishes at far below the Curie temperature. Several models have been proposed to explain the CMR phenomenon. One is the double-exchange model [Zener 51a, Zener 51b]: the spin fluctuations get reduced upon the application of a magnetic field, leading to the increase in conductivity. This model is generally true for the suppression of spin fluctuations in ferromagnetic metals. However, this model can not alone either explain the CMR phenomenon or predict the magnitude of the CMR effect [Millis 95]. Another model [Millis 98] includes the polaron formation near the metal-insulator transition temperature. It claims that the strong electron-phonon coupling leads to the metal-insulator transition. Experimentally, there is evidence for a formation of polarons near the metal-insulator transition temperature [Worledge 96, De Teresa 98] in manganite materials.

Double exchange plus electron-phonon interaction together can explain the occurrence of a metal-insulator transition. But no model could explain the large CMR effect of low- $T_C$  manganites yet. The debate on explaining the CMR effect still goes on, which includes phase separation and critical fluctuation models from Dagotto [Dagotto 01], Murakami and Nagoasa [Murakami 03]. Dagotto describes a model based on a percolation mechanism. The existence of metallic and insulating regions with different electrical conductivities is assumed. The total conductivity is the resultant of electrical conductivities of the metallic and insulating phase separated regions and their spatial arrangement. Murakami and Nagoasa suggest a model based on enhanced fluctuations near a multicritical point.

### 1.3 Extrinsic phenomena

In the previous section on intrinsic transport properties, the typical behavior of single crystals and epitaxial films has been discussed. This section deals with the introduction to effects that originate from defects, grain boundaries and domain walls to the resistance (R) and MR. Grain boundaries are present in polycrystalline ceramic compounds with typical grain sizes from 100 nm to 10  $\mu\text{m}$  in both

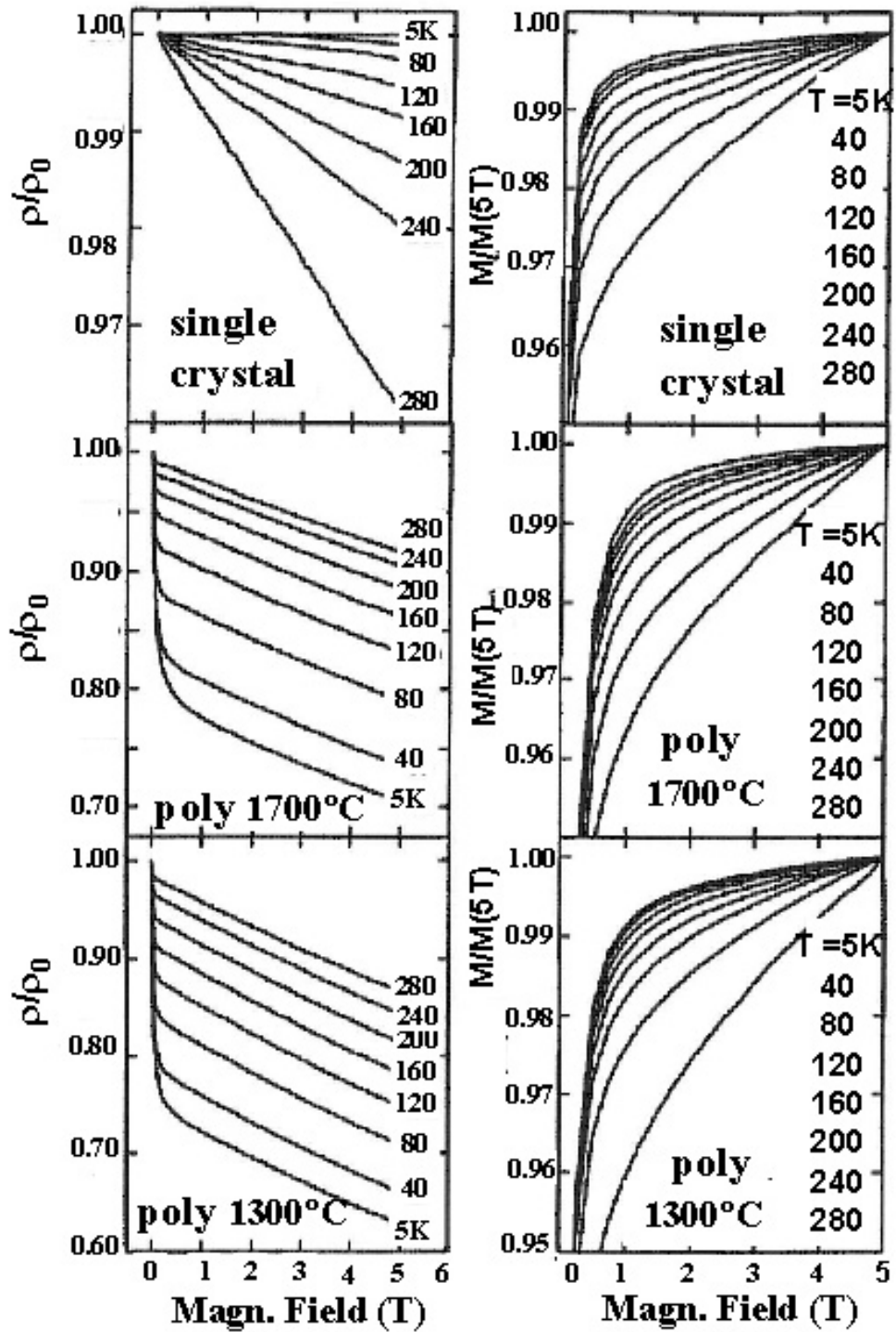


Figure 1.5: Magnetic field dependences of the normalized resistivity and of the magnetization (normalized to the value at 5 T) at various temperatures for single crystalline and polycrystalline  $\text{La}_{0.67}\text{Sr}_{0.33}\text{MnO}_3$  [Hwang 96].

thin films and in bulk compounds. A single grain boundary can be obtained by growing an epitaxial film on a bicrystal substrate. Other ways to obtain extended defects or grain boundaries are by depositing an epitaxial film over sharp steps in the substrate or on scratched substrates.

In the pioneering work of Hwang et al. [Hwang 96], field dependent magnetization and magnetoresistance data measured at different temperatures for bulk single crystalline and two bulk polycrystalline samples of  $\text{La}_{0.67}\text{Sr}_{0.33}\text{MnO}_3$  have been compared, see Fig.1.5. The polycrystalline manganite sintered at high temperature ( $1700^\circ\text{C}$ ) shows a larger grain size compared to the manganite sintered at lower temperature ( $1300^\circ\text{C}$ ). From Fig.1.5, it is obvious that the change in magnetization with applied magnetic field is the same for both single crystal and polycrystalline manganite. In contrast, the magnetoresistance deviates considerably. At low temperature, there is a 20 - 35% reduction in the resistance in low magnetic fields and a continuous further drop in high magnetic fields for the polycrystalline compounds. The drop in resistance at low fields for polycrystalline manganites vanishes at high temperatures. For single crystalline manganites, the magnetoresistance is maximum near the metal-insulator transition temperature and decreases towards low temperature (see section 1.2). Hwang et al. [Hwang 96] suggested that the low field magnetoresistance in polycrystalline samples is due to spin-polarized tunneling between mis-aligned grains. In recent years, the low-field magnetoresistance has drawn much attention to utilize this effect for magnetic sensors. There were many attempts to increase the drop in resistance towards high temperatures. Balcells et al. [Balcells 98] studied the systematic dependence of the magnetoresistance on grain size. They observed that the low-field effect increases with decreasing grain size.

Experimentally, there is no versatile technique which can probe directly the grain boundary magnetism. The electric and magnetotransport measurements are utilized to understand the grain boundary effects. Hence, from the grain boundary transport measurements, some generalized conclusions have been drawn. The transport characteristics of grain boundaries indicates,

- a drop in resistance at low magnetic field of the order of the magnetic coercive field,
- a non-vanishing high-field magnetoresistance at fields  $\mu_0 H > 1 \text{ T}$ ,
- nonlinear current-voltage characteristics.

---

Experimentally, other defects than grain boundaries are found to show similar transport features, like the drop in the resistance at low fields and a non-vanishing high field MR. The magnitude of the low-field effect is found to be dependent on the grain boundary angle [Paranjape 03]. In search of finding the magnitude with respect to the grain boundary angle, other effects like domain wall scattering comes into the picture, especially in single grain boundary junctions. Wagenknecht et al. [Wagenknecht 06] could show the nucleation and growth of magnetic domains near the grain boundary in single grain boundary junctions using a low temperature scanning laser microscope.